PAPER

CT organ dose calculator size adaptive for pediatric and adult patients

To cite this article: Choonsik Lee *et al* 2022 *Biomed. Phys. Eng. Express* **8** 065020

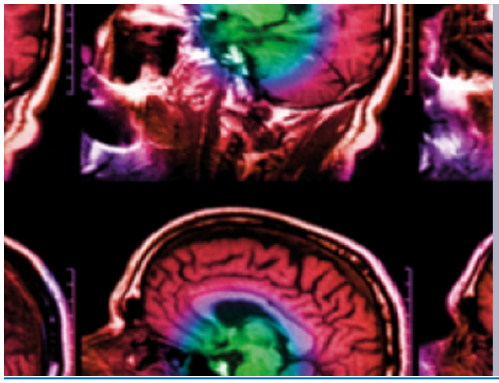

Biomedical Physics & Engineering Express

PAPER

CT organ dose calculator size adaptive for pediatric and adult patients

RECEIVED
6 April 2022

REVISED
12 September 2022

ACCEPTED FOR PUBLICATION
7 October 2022

PUBLISHED
19 October 2022

Choonsik Lee[1,*], **Yeon Soo Yeom**[2] and **Les Folio**[3]

[1] Division of Cancer Epidemiology and Genetics, National Cancer Institute, National Institutes of Health, Rockville, MD, United States of America
[2] Department of Radiation Convergence Engineering, Yonsei University, Wonju, Republic of Korea
[3] Moffitt Cancer Center, Tampa, FL, United States of America
[*] Author to whom any correspondence should be addressed.

E-mail: choonsik.lee@nih.gov

Keywords: phantoms, dose, organ, pediatric, adult, patients

Abstract

Background. Although computed tomography (CT) has played a critical role in medical care since its introduction in the 1970s, its potential long-term risk of adverse health effects has been of concern. It is crucial to accurately estimate the radiation dose delivered to the patient's critical organs to ensure the dose is As Low As Reasonably Achievable. However, organ-level dose calculation tools for pediatric and adult patients with various body sizes are rare. We extended the existing CT organ dose calculator, NCICT 1.0, which is based on reference-size phantoms, to include body size-specific pediatric and adult phantoms. *Methods*. We calculated body size-specific organ doses normalized to $CTDI_{vol}$ by using a library of 158 pediatric and 193 adult computational human phantoms with various body sizes combined with a Monte Carlo radiation transport code, MCNP6. We also created a library of generic tube current modulation (TCM) profiles for the phantom library using a ray-tracing algorithm and implemented them into organ dose calculations. We validated organ doses for the body size-specific phantoms using those calculated from ten abdominal CT patients. We also evaluated potential dosimetric errors caused by only using reference phantoms for patients with different body sizes. *Results*. Organ dose coefficients and TCM profiles for 351 pediatric and adult body size-specific phantoms were implemented into NCICT 2.0. The dose coefficients from the ten abdominal CT patients agreed with those from the program within 13%. The organ doses for the overweight phantoms were overestimated by over 80% when only reference size phantoms were used. *Conclusion*. We confirmed that the upgraded dose calculator NCICT 2.0 could substantially reduce potential dosimetric errors caused by using only reference size phantoms. The program should be useful for the radiology community to accurately monitor organ doses for pediatric and adult CT patients with various body sizes.

Introduction

Although computed tomography (CT) has played a critical role in medical care since its introduction in the 1970s, the long-term risk of adverse health effects potentially caused by CT radiation exposure has been of concern [1–3]. It is crucial to accurately estimate the radiation dose delivered to CT patients to ensure the dose is As Low As Reasonably Achievable 4. Some dose metrics are available from CT scanners, such as volume computed tomography dose index ($CTDI_{vol}$) and dose length product (DLP) but are not the dose delivered to a patient's organs, which is the most fundamental quantity for risk analysis 5. Several patient-specific factors, such as patient age, gender, and body size, have substantial dosimetric impacts, so they must be considered for accurate dose estimation for CT patients.

Computer simulation is one of the efficient methods to estimate organ-level doses for CT patients. The method uses CT scanner simulation models with digital human anatomy models, called computational human phantoms 6. Detailed technical parameters involved in CT scans are implemented into computer simulations,

often based on Monte Carlo radiation transport techniques. A library of dose conversion coefficients for different combinations of CT parameters can be precalculated and implemented into computer software with a graphical user interface. Several CT dose calculators are available based on the pediatric and adult computational human phantoms with reference body size [7–10], including the National Cancer Institute dosimetry system for Computed Tomography (NCICT) 11. However, organ doses may substantially vary by the size of patients, even within the same age groups. To account for the body size in organ dose estimation, Ding *et al* 12 developed the VirtualDose tool by implementing a library of ten adult male and female phantoms representing the Body Mass Index (BMI) from 24 to 46 kg-m^{-2}. However, the tool does not consider the variation in body size for pediatric patients. Tian *et al* 13 developed regression models to predict organ dose for chest and abdomen-pelvis (AP) scans by using a library of patient-specific phantoms consisting of 42 pediatric patients with various body sizes. The methods can estimate organ-level dose for chest or AP scans using patient diameters but are not applicable to other scan coverages and cases where the patient diameter is unavailable.

To fill the research gap, we extended the existing CT organ dose calculator, NCICT version 1.0 11, based on twelve reference size pediatric and adult phantoms, to include the pediatric and adult phantoms with a variety of heights and weights 14. A comprehensive dose library and longitudinal tube current modulation (TCM) profiles were created using the phantoms and then implemented into the NCICT version 2.0. We described the updated dose calculator and showed how it could substantially reduce potential dosimetric errors commonly occurring when using only reference-size phantoms.

Materials and methods

Computational human phantoms

We adopted a library of pediatric and adult computational human phantoms with various body sizes developed in collaboration between the University of Florida and the National Cancer Institute 14. The phantom library includes pediatric female (n = 73) and male (n = 85) phantoms with a range of heights (85–185 cm) and weights (10–125 kg) (figure 1(A)) and adult female (n = 93) and male (n = 100) phantoms with a range of heights (150–190 cm) and weights (40–140 kg) (figure 1(B)). The phantom library was developed by morphing a series of twelve pediatric and adult reference size phantoms 15 by adjusting the seven anthropometric data (height, weight, sitting height, and the circumference of waist, thigh, arm, and buttocks) based on the NHANES IV 1999–2006 database. Each phantom includes over 80 organs and tissues segmented from patient CT images. Cortical and spongiosa bones are separately modeled in 35 different bone sites for accurate estimation of active marrow and endosteum doses.

To realistically simulate the arm posture of CT patients in both head (arms lowered) and torso (arms raised) scans, the arms were removed from the phantoms. We kept the humeral heads in the upper shoulders, which contain a significant amount of active marrow 16 and are likely to be included in the scan coverage of the head or torso scans. The original phantoms in Non-uniform Rational B-Spline (NURBS) and polygon mesh format were converted to voxel format for Monte Carlo radiation transport using the voxel resolutions ranging from 0.0003 cm^3 (newborn) to 0.0055 cm^3 (adult male). We converted the binary voxel format to lattice files in ASCII format for Monte Carlo transport simulations.

Body size-specific organ dose conversion coefficients

We used a general-purpose Monte Carlo radiation transport code, MCNP6, to simulate the interaction of x-rays within the reference CT scanner model and the computational human phantoms. A total of 10 million particle histories were used to reduce the Monte Carlo errors for in- and near-field organs to less than 1%. We utilized the high-performance computing server available at the US National Institutes of Health to conduct a large number of Monte Carlo dose calculations.

We calculated organ doses normalized to $CTDI_{vol}$, called scanner-independent organ dose conversion coefficients [17, 18] (mGy mGy^{-1}), using the Monte Carlo simulation model of a reference CT scanner combined with the computational human phantom library. The CT scanner simulation model was previously validated by the measurements using CTDI phantoms 11 and physical anthropomorphic phantoms [18–20]. We calculated organ doses by simulating each computational phantom exposed to a fan-shaped rotating CT x-ray beam with a 1 cm consecutive vertical increment from the top of the head to the bottom of the feet of the phantoms (e.g., 170 slices for 170 cm high adult male phantom). The calculation was repeated for a total of eight x-ray spectra (combination of 80, 100, 120, and 140 kVp, and head and body filters). For the adult phantoms (n = 193) exposed to the x-ray spectrum of 120 kVp with the body filter, we adopted the organ dose coefficients previously calculated for another study 21.

The radiation dose delivered to 31 organs and tissues was calculated: brain, pituitary gland, lens, eyeballs, salivary glands, oral cavity, spinal cord, thyroid, esophagus, trachea, thymus, lungs, breast, heart wall, stomach wall, liver, gallbladder, adrenals, spleen, pancreas, kidney, small intestine, colon, rectosigmoid, urinary bladder, prostate, uterus, testes, ovaries, skin, and muscle. Assuming that charged particle equilibrium is established for the x-ray energy less than 140 kVp, kerma was calculated without tracking

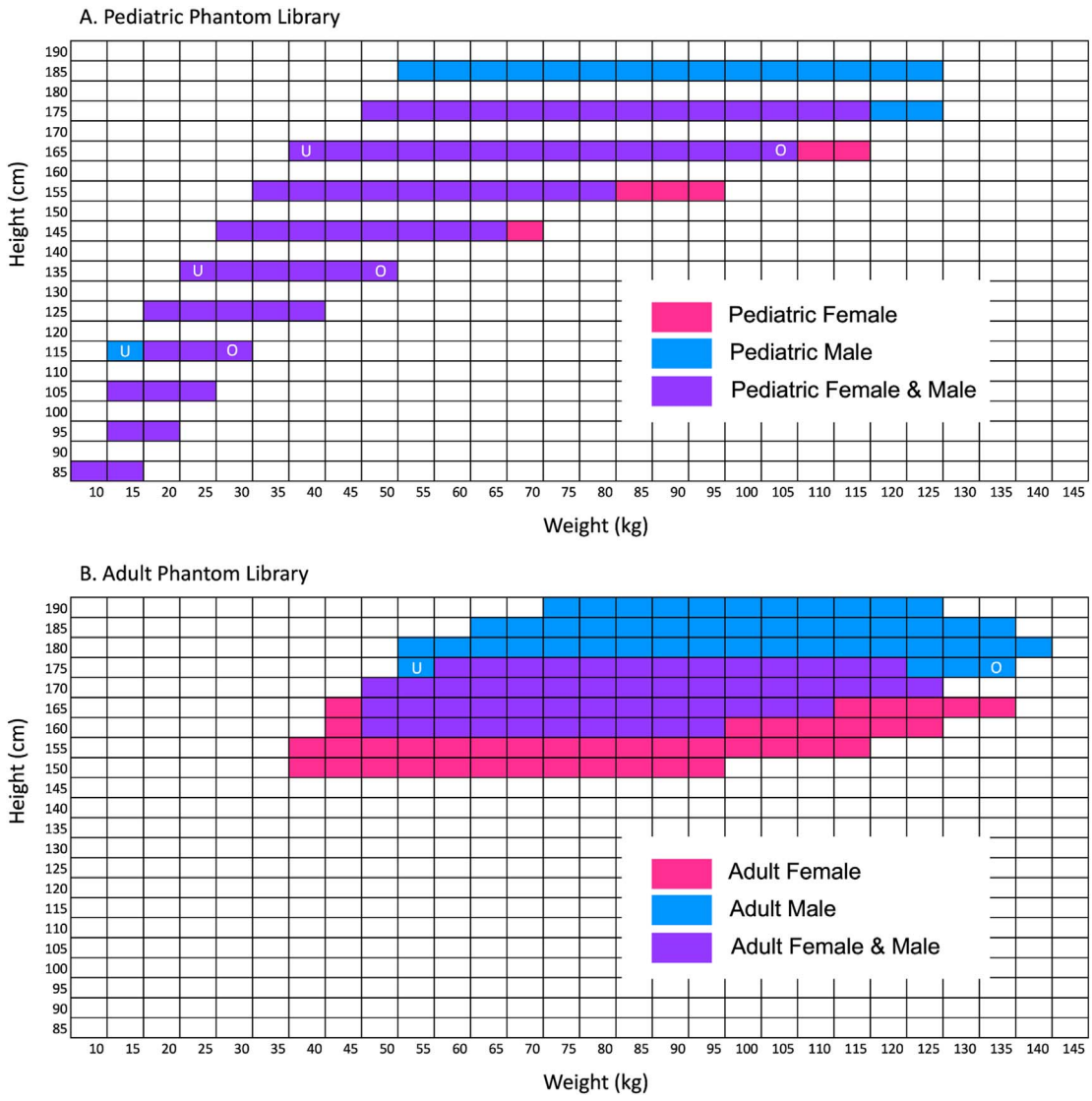

Figure 1. Distribution of the height (cm) and weight (kg) of the (A) pediatric male and female and (B) adult male and female computational phantoms adopted in NCICT 2.0. The male phantoms representing underweight (U) and overweight (O) used for dose comparison are labeled for the reference heights of 115, 135, 165, and 175 cm for 5, 10, 15 years, and adult age groups, respectively.

secondary electrons, substantially reducing calculation time. Active marrow and endosteum doses were calculated from the fluence scored in the spongiosa region of 31 bone sites (after removing arms) using skeletal dose response function [22, 23]. The effective dose was calculated using the organ doses combined with the tissue weighting factors published in ICRP Publication 103 24. It must be noted that effective dose was derived only for a given gender (male or female) which is not exactly following its definition by ICRP 24.

Validation of phantom-based organ dose using patient CT

We validated the organ doses calculated from the body size-specific phantoms with those calculated from ten CT patients (five males and five females) with different body sizes. Convenient samples of anonymized patient abdominal CT images were collected from the National Institutes of Health Clinical Center under an Institutional Review Board-exempt study protocol. We adopted in-house automatic segmentation methods based on a Multi-Atlas Label Fusion technique [25, 26] to segment major thoracic and abdominal organs from the CT images: liver, left and right kidneys, spleen, pancreas, and lungs. The same Monte Carlo simulation methods described in the previous section were used to calculate patient-specific organ doses. The effective diameter of the patients measured at the mid-level of the CT coverage ranged from 23 to 33 cm. Details about the image segmentation and dose calculation process were published elsewhere 27.

To compare the organ doses between the ten patients and the body size-specific phantoms, we derived fitting curves between effective diameters and organ dose coefficients for eleven phantoms matching the height of 175 cm (close to the reference height of adults assumed for both patients and phantoms) with a range of

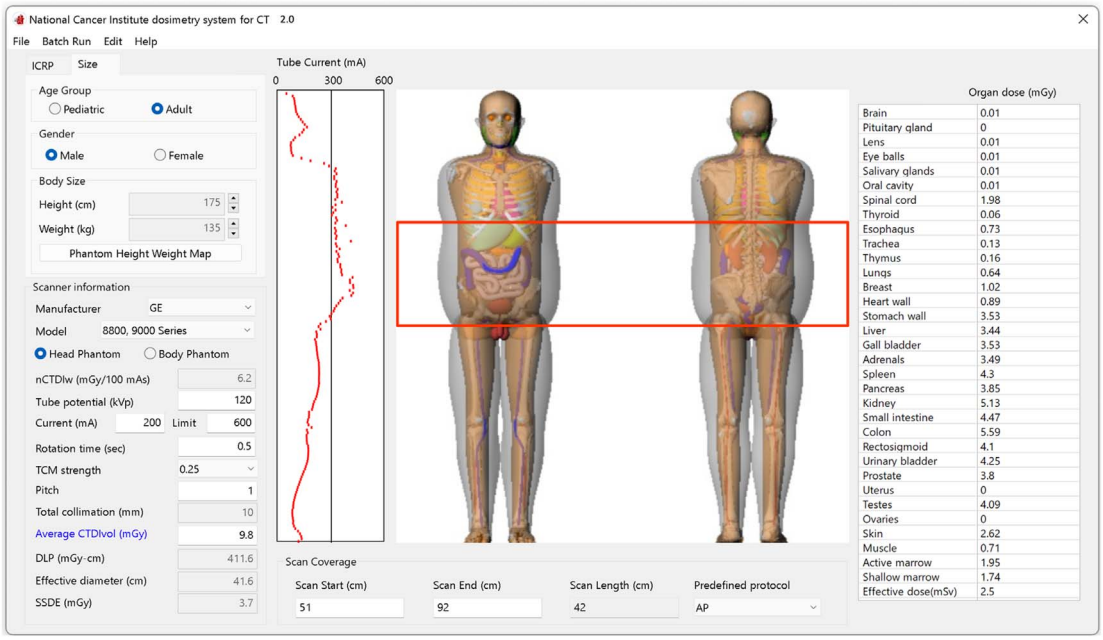

Figure 2. The graphical user interface of NCICT 2.0 where CT technical parameters and patient information are entered to calculate organ-specific doses for a male pediatric patient with a height of 175 cm and a weight of 135 kg in abdominal-pelvis CT scans selected.

abdominal effective diameters covering those of the ten patients. We evaluated how well the phantom-based fitting curves predict patient-specific doses for the liver, kidneys, spleen, and pancreas by calculating prediction errors represented by Mean Absolute Percent Error (MAPE) (%). We also calculated R^2 across the ten patients for those four organs to evaluate the degree of variability among the patients.

Tube current modulation profiles

We adopted the method reported by Li *et al* 28 to calculate modulated tube current based on reference tube current and attenuation ratio:

$$I(z) = I_{ref} \times \left(\frac{A_z}{A_{ref}}\right)^{\alpha} \quad (1)$$

where $I(z)$ is the modulated tube current (mA) at the longitudinal location z, I_{ref} is a reference tube current (mA), A_z is the attenuation at the longitudinal location z (initial intensity per attenuated intensity), A_{ref} is an attenuation of x-ray passing through a reference water phantom (34 cm thick) at the center of the bowtie filter, and α is the theoretical TCM strength ranging from zero to unity. Attenuation averaged within the fan beam angle was calculated with the interval of five-degree rotational gantry angle surrounding the beam isocenter. The fan beam angle-averaged attenuation (angular modulation) was averaged over 360-degree gantry angles for a single slice, so only longitudinal modulation was taken into account. We calculated the TCM profiles for the 351 body size-specific phantoms and 12 reference size ICRP phantoms for the x-ray spectra at 80, 100, 120, and 140 kVp with the head filter. The profiles for the body filter were very similar to those for the head filter.

User interface update

To receive the user input data and calculate absolute organ doses D_{organ} (mGy) using the library of organ dose conversion coefficients (mGy mGy^{-1}) and TCM profiles, we implemented the following two equations into the graphical user interface-based program. First, if $CTDI_{vol}$ is available from CT scanners, the value can be directly entered into the user interface for dose calculations. However, if unavailable, $CTDI_{vol}$ must be calculated using the following equation and technical parameters:

$$CTDI_{vol}(spectrum, CTDI\ phantom, z) = \frac{nCTDI_w(spectrum, CTDI\ phantom)}{Pitch} \times I(z) \times t \times k_{OB} \quad (2)$$

where $CTDI_{vol}(spectrum, CTDI\ phantom, z)$ is the $CTDI_{vol}$ for a specific x-ray spectrum, CTDI phantom, and the longitudinal location z, $nCTDI_w$ is the normalized $CTDI_w$ (mGy mAs^{-1}) specific to a user-selected CT scanner model and CTDI phantom type 29, *Pitch* is the pitch factor, $I(z)$ (mA) is the modulated tube current calculated from equation (1) at the longitudinal location z, t (second) is a single rotation exposure time, and k_{OB} is the overbeaming correction factor defined by Nagel *et al* 30. Second, absolute organ dose D_{organ} (mGy) was then calculated using the following equation:

$$D_{organ} = \sum_{z=SS}^{z=SE} \frac{D_{MC}(organ, phantom, spectrum, z)}{CTDI_{vol,MC}(spectrum, CTDI\ phantom, z)} \times CTDI_{vol}(spectrum, CTDI\ phantom, z) \quad (3)$$

where z is the slice number ranging from 1 to the total number of slices (equivalent to the height of a

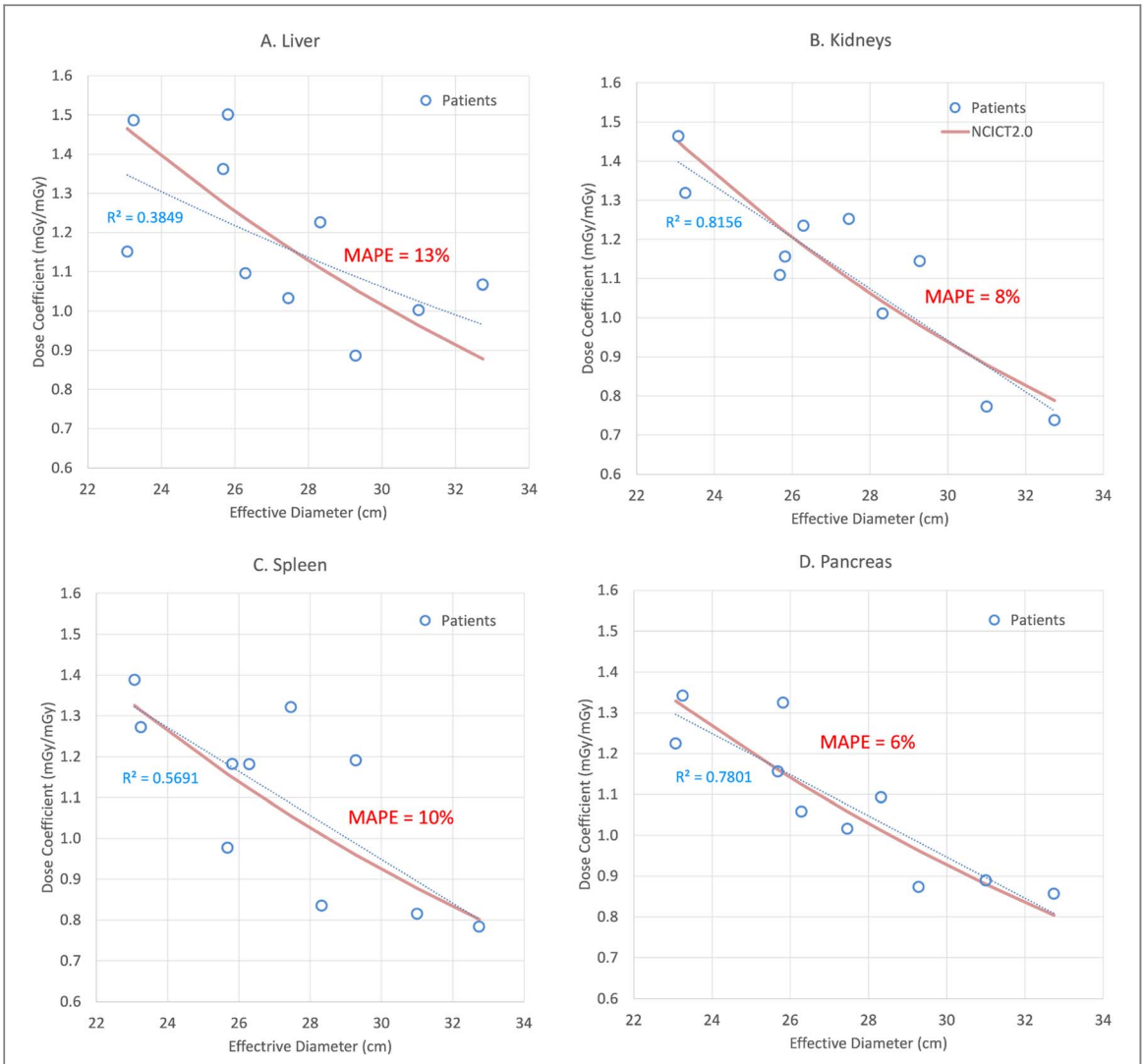

Figure 3. Comparison of organ dose coefficients (mGy/mGy) for different effective diameters (cm) between CT image-based patient models and NCICT2.0 for (A) liver, (B) kidneys, (C) spleen, and (D) pancreas.

phantom in cm) with 1 cm interval, *phantom* is selected by patient height and weight, *SS* is the slice number at the scan start, *SE* is the slice number at the scan end, $D_{MC}(organ, phantom, spectrum, z)$ (mGy photon^{-1}) is organ dose per launched photon calculated from Monte Carlo simulation as a function of the organ, phantom, x-ray spectrum, and slice number, $CTDI_{vol,MC}$ is the $CTDI_{vol}$ per launched photon (mGy photon^{-1}) calculated from the Monte Carlo simulation of the reference CT scanner as a function of x-ray spectrum and CTDI phantom size (16 cm or 32 cm diameter), and $CTDI_{vol}(spectrum, CTDI\ phantom, z)$ is the value calculated from equation (2).

Effective diameter (cm) was precalculated for the body size-specific phantoms with the 1-cm longitudinal interval from the top of the head to the bottom of the feet. The results were used to derive Size Specific Dose Estimates (SSDE) according to the method reported by AAPM TG204 31.

To obtain user input data and display organ dose results for the new size-specific phantom library with TCM profiles, we created three new user interfaces. First, we implemented a menu for users to select body size-specific computational human phantoms based on age group (pediatric or adult), gender (male or female), height, and weight. To help select the height and weight available from the phantom library, we created the height and weight distribution maps for the pediatric and adult female and male groups. Second, we separated reference tube current (mA), I_{ref}, as described in equation (1), and rotation time (second), t, which were previously combined into tube current-time-product (mAs) . The tube current modulation was applied to a user-provided reference tube current, which was then used to derive modulated $CTDI_{vol}$ as desribed in equation (2). Users can enter the machine limit of tube current (default value is 600 mA), which prevents the over-modulation of tube current for overweight phantoms. Finally, we created a menu for users to choose a hypothetical TCM strength α as described in equation (1), ranging from zero to unity.

NCICT 1.0 provides the batch dose calculation function 11 to facilitate dose calculations for a large number of patients. Users can create multiple lines of the patient-

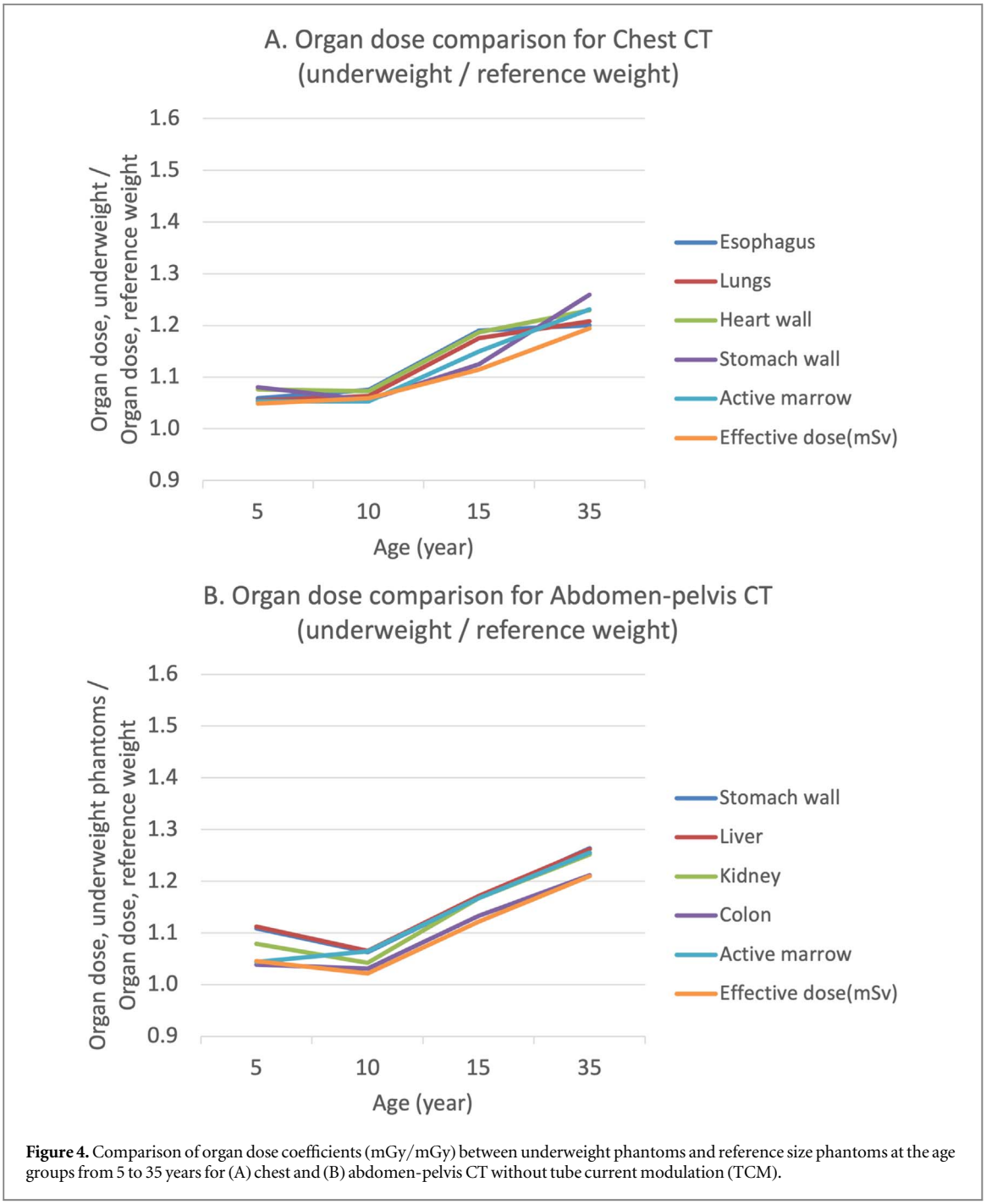

Figure 4. Comparison of organ dose coefficients (mGy/mGy) between underweight phantoms and reference size phantoms at the age groups from 5 to 35 years for (A) chest and (B) abdomen-pelvis CT without tube current modulation (TCM).

related and CT technical parameters in comma-separated values (CSV) format. The program can import the CSV file, calculate organ doses for each line representing a single CT exam, and export organ and effective doses in a CSV file. The input parameters include patient ID, scan start location (cm), scan end location (cm), $CTDI_{vol}$, patient age, patient gender, tube potential (kVp), and beam filter type (head or body). To facilitate the new organ dose calculation algorithm described in equations (1)–(3) in the batch module, input parameters were modified: patient ID, scan start location (cm), scan end location (cm), phantom group (1-pediatric female, 2-pediatric male, 3-adult female, and 4-adult male), height (cm), weight (kg), tube potential (kVp), TCM strength (0, 0.25, 0.5, 0.75, and 1), CTDI phantom type (1–16 cm head phantom, 2–32 cm body phantom), and average $CTDI_{vol}$ (mGy).

To resolve the packaging issues with NCICT 1.0 written in Python, we completely recreated the graphical user interface and dose calculation routines using a multi-platform computer language, Xojo (Xojo Inc., Austin, Texas). The language allowed the program for running on multiple operating systems such as Windows, Mac, LINUX.

Evaluation of dosimetric errors by reference phantoms

We evaluated potential dosimetric errors caused by only using reference phantoms (available in NCICT

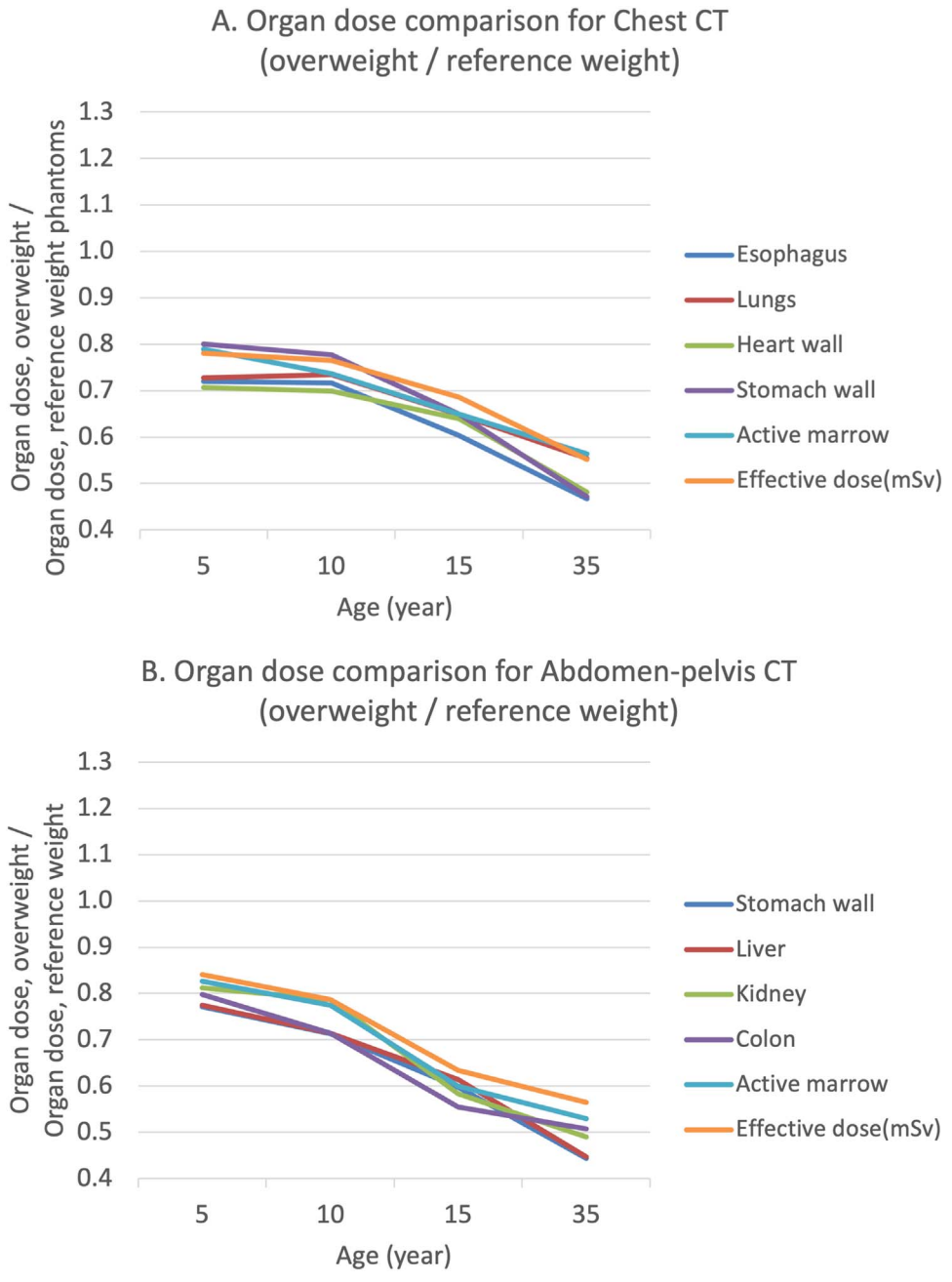

Figure 5. Comparison of organ dose coefficients (mGy/mGy) between overweight phantoms and reference size phantoms at the age groups from 5 to 35 years for (A) chest and (B) abdomen-pelvis CT without tube current modulation (TCM).

Table 1. TCM-based average $CTDI_{vol}$, lung and colon doses in chest and abdomen-pelvis CT, respectively, calculated using underweight and overweight phantoms at the heights of 115, 135, 165, and 175 cm and reference size phantoms. Percent errors (%) were calculated between size-specific phantoms and reference-size phantoms in different height categories.

Organ in CT scan type	Age group	5 years		10 years		15 years		35 years	
	Height (cm)	115 cm		135 cm		165 cm		175 cm	
	Weight (kg)	15 kg	30 kg	25 kg	50 kg	40 kg	105 kg	55 kg	135 kg
Lung dose in Chest CT	Average $CTDI_{vol}$ (mGy)	2.70	3.90	3.10	4.60	3.40	6.80	2.30	5.30
	Size-specific phantom	2.59	2.61	2.64	2.62	3.21	3.79	3.51	3.77
	Reference phantom	2.48	3.59	2.45	3.63	2.52	5.03	2.99	6.89
	Errors (%)	−4.09	37.47	−7.23	38.70	−21.62	32.77	−14.81	82.76
Colon dose in AP CT	Average $CTDI_{vol}$ (mGy)	2.70	3.90	3.20	4.50	3.60	6.90	2.40	5.50
	Size-specific phantom	2.95	3.08	3.14	3.25	3.32	3.27	3.85	4.14
	Reference phantom	2.81	4.06	3.04	4.51	2.82	5.64	3.27	7.53
	Errors (%)	−4.81	31.69	−3.25	38.71	−15.00	72.60	−15.17	81.79

1.0) for patients with different body sizes in two ways: (1) comparison of $CTDI_{vol}$-normalized organ doses without TCM between reference size and size-specific phantoms to investigate the impact of anatomical difference only, and (2) comparison of absolute organ doses with TCM between reference size and size-specific phantoms.

First, we compared $CTDI_{vol}$-normalized organ doses from reference size phantoms with those from the underweight and overweight male phantoms at different age groups: 5, 10, 15 years, and adults. For example, we compared organ doses per $CTDI_{vol}$ from the two size-specific phantoms with weights of 25 (underweight) and 50 (overweight) at the height of 135 cm (reference height of a 10-year-old child 16) with those from the 10-year-old reference child phantom. In figure 1, the male phantoms representing underweight (U) and overweight (O) used for dose comparison are labeled for the reference heights of 115, 135, 165, and 175 cm for 5, 10, 15, and 35 (adult)-year-old, respectively.

Second, we compared TCM-implemented absolute organ doses between reference size phantoms and the same underweight and overweight size-specific phantoms used for the abovementioned comparison. The underweight and overweight phantoms were selected as described above (figure 1). We first calculated the average $CTDI_{vol}$ for chest and abdomen-pelvis CT scans from slice-specific $CTDI_{vol}$ from each phantom. The lung dose for chest CT and colon dose for abdomen-pelvis scan were then calculated using the two sets of organ dose conversion coefficients derived from the size-specific phantoms and the reference size phantoms multiplied by the average $CTDI_{vol}$ values. Scan parameters were set as follows: reference tube current of 200 mA, tube current limit of 600 mA, tube potential of 120 kVp, rotation time of 0.5 seconds, pitch of 1, and TCM strength of 0.25.

Results

NCICT 2.0 user interface

Figure 2 shows the graphical user interface of NCICT 2.0, composed of four panels from left to right: patient information, scanner information, scan coverage, and organ dose output. First, a user has two options for a phantom library: 'ICRP' reference size phantoms and 'Size' specific phantoms. When the ICRP panel is selected, users can choose age group (0, 1, 5, 10, 15-year-old, and adult) and gender. When the Size panel is selected, users can input age group (pediatric or adult), gender, and the height and weight of a patient referring to the height and weight maps. Whenever a phantom is selected, the frontal and rear views are shown in the mid-panel. Second, when the scanner model and CTDI phantom type are specified in the scanner information panel, the corresponding normalized $CTDI_w$ (mGy mAs^{-1}) is displayed. When users input tube potential, tube current, rotation time, TCM strength, and pitch, the average $CTDI_{vol}$ is automatically calculated. To define scan coverage on the third panel, users can drag the mouse pointer on the phantom picture or manually enter the scan start and end location (cm) or select a predefined scan protocol (head, neck, chest, abdomen, pelvis, abdomen-pelvis, and chest-abdomen-pelvis). The predefined scan coverage is automatically adjusted to match the corresponding anatomical landmarks of phantoms with different heights. Lastly, the organ dose panel displays the absolute organ dose (mGy) and effective dose (mSv). NCICT2.0 is packaged and distributed in the two installation formats running on Windows and Mac.

Validation of phantom-based organ dose using patient CT

MAPE (%) in the dose coefficients (mGy mGy^{-1}) between the patients (observed) and NCICT 2.0 (predicted) was 13%, 8%, 10%, and 6% for the liver, kidneys, spleen, and pancreas, respectively (figure 3). R^2 derived from the patient-specific organ doses was 0.38, 0.82, 0.57, and 0.78 for the liver, kidneys, spleen, and pancreas, respectively.

Dosimetric errors by using reference size phantoms

When TCM was not implemented and organ doses were normalized to $CTDI_{vol}$, the reference phantoms underestimated organ doses for chest CT from underweight phantoms by up to 8%, 8%, 19%, and 25% for the age groups of 5, 10, 15 years, and adult, respectively (figure 4(A)). The underestimation of organ doses for the underweight phantoms by reference phantoms for AP CT was by up to 11%, 6%, 17%, and 26% for 5, 10, 15 years, and adult, respectively (figure 4(B)). Reference phantoms overestimated organ doses for overweight phantoms for chest CT by up to 29%, 30%, 40%, and 53% (figure 5(A)) and for AP CT by up to 23%, 29%, 45%, and 56% (figure 5(B)), for 5, 10, 15 years, and adult, respectively. The dosimetric errors increased when the age group increased.

When TCM was implemented into dose calculations, the reference phantoms underestimated the lung and colon doses of the underweight phantoms by up to 22% and 15% (15 years group), respectively (table 1). The lung and colon doses for the overweight phantoms were overestimated by up to 83% and 82% (35 years group), respectively, when only reference phantoms were used. The underestimation errors increased from about 4% to 15% (lung dose in chest CT) when the age group increased from 5 to 35 years. With increasing age groups, the overestimation errors also increased from 37% to 83% (lung dose in chest CT).

Discussion

Among different dose descriptors derived for CT patients, organ absorbed dose is the essential quantity directly relevant to estimating the risk of adverse health effects 5. The impact of body size on patient doses in CT is widely recognized [31, 32], but few organ dose calculation tools are available for pediatric and adult patients with various body sizes. We upgraded NCICT 1.0 (only reference size phantoms available without TCM) to 2.0 by implementing the comprehensive library of dose coefficients and TCM profiles calculated from the body size-specific pediatric and adult phantom library (n = 351).

The body size-specific organ dose conversion coefficients from the upgraded program were validated using CT image-based organ doses of ten patients with various body sizes. The two sets of organ doses agreed well (the MAPE less than 13% (figure 3)). R^2 values (the degree of individual variability) were inversely correlated with the MAPEs, indicating that the prediction errors by the program decreased when the inter-patient dose variation decreased (increasing R^2).

NCICT 1.0 only provides reference size ICRP phantoms based on age group without TCM, and $CTDI_{vol}$ is fixed across the longitudinal scan locations without modulation. The difference in organ dose conversion coefficients between size-specific phantoms and reference size phantoms (figure 4) represents the dosimetric errors when only reference phantoms are used for patients with various body sizes by selecting phantoms only based on patient age and ignoring TCM. Dosimetric errors over 25% for underweight and 50% for overweight patients can be addressed by using the upgraded program.

When TCM was implemented, the dosimetric errors caused by using only reference phantoms further increased up to 80%, especially for overweight phantoms because $CTDI_{vol}$ now increased by body size. $CTDI_{vol}$ increased by 2.3-fold when body size increased from underweight to overweight phantoms (table 1). This finding agrees with Barreto *et al* reporting that $CTDI_{vol}$ increases exponentially with the effective diameter of patients [33]. The dosimetric errors increased as the age group of phantoms increased because the variability in body size was greater in older phantoms than in younger ones, as shown in the breadth of weight distribution at the same height (figure 1).

We are aware that the current study has the following limitations. First, we acknowledge that although our size-specific phantoms improved dosimetric accuracy for patients with non-standard body sizes, anatomical discrepancy still exists between patients and phantoms. New approaches to combine auto-segmented patients' anatomy with pre-segmented human phantoms may fill the gap [34]. Second, the body size-specific organ dose coefficients were validated by CT image-based organ doses for adult patients. The validation may be extended to pediatric patients with various body sizes in the future. Lastly, the TCM-based organ doses proposed in the current study are based on a generic modulation model with the theoretical TCM strength. Further studies are required to compare the theoretical current modulations with those based on vendor-specific TCM algorithms.

Conclusion

We upgraded an existing dose calculator by implementing body size-specific organ dose coefficients and TCM profiles calculated using a total of 351 pediatric and adult male and female computational human phantoms. We found that the organ doses for the overweight phantoms could be overestimated by over 80% when only reference-size phantoms were used. We confirmed that the new dose calculator NCICT 2.0 could substantially reduce potential dosimetric errors caused by ignoring body size in dose calculations. The program should be useful for the radiology community to accurately monitor organ doses for pediatric and adult CT patients with various body sizes. The program is available from http://ncidose.cancer.gov free of charge for research purposes.

Acknowledgments

This research was funded by the intramural research program of the National Institutes of Health (NIH), National Cancer Institute, Division of Cancer Epidemiology and Genetics. This work utilized the computational resources of the NIH High-Performance Computing Biowulf cluster (http://biowulf.nih.gov).

Data availability statement

The data that support the findings of this study are openly available at the following URL/DOI: https://dceg.cancer.gov/tools/radiation-dosimetry-tools.

ORCID iDs

Choonsik Lee https://orcid.org/0000-0003-4289-9870
Yeon Soo Yeom https://orcid.org/0000-0001-5373-6693

References

[1] Pearce M S *et al* 2012 Radiation exposure from CT scans in childhood and subsequent risk of leukaemia and brain tumours: a retrospective cohort study *Lancet* **380** 499–505
[2] Meulepas J M *et al* 2019 Radiation exposure from pediatric CT scans and subsequent cancer risk in the Netherlands *J Natl Cancer Inst.* **111** 256–63
[3] Mathews J D *et al* 2013 Cancer risk in 680,000 people exposed to computed tomography scans in childhood or adolescence: data linkage study of 11 million Australians *Br Med J.* **346** f2360

[4] ICRP 1991 1990 Recommendations of the international commission on radiological protection. *ICRP Publ 60 Ann ICRP* **21** 1–3
[5] Harrison J D *et al* 2021 ICRP Publication 147: use of dose quantities in radiological protection *Ann. ICRP* **50** 9–82
[6] Xu X G 2014 An exponential growth of computational phantom research in radiation protection, imaging, and radiotherapy: a review of the fifty-year history *Phys. Med. Biol.* **59** R233–302
[7] ImPACT 2011 *ImPACT CT Patient Dosimetry Calculator [Internet]*. (London, UK) Available from (http://impactscan.org/ctdosimetry.htm)
[8] Stamm G and Nagel H D 2002 CT-Expo–a novel program for dose evaluation in CT. ROFO *Fortschr. Geb. Rontgenstr. Nuklearmed.* **174** 1570–6
[9] CT Imaging 2015 *ImpactDose 2.2 [Internet]*. (Erlangen, Germany: CT Imaging GmbH) Available from (http://ct-imaging.de/images/Downloads/impactdose_user manual.pdf)
[10] Lee C 2021 A review of organ dose calculation tools for patients undergoing computed tomography scans *J Radiat Prot Res* **46** 151–9
[11] Lee C, Kim K P, Bolch W E, Moroz B E and Folio L 2015 NCICT: a computational solution to estimate organ doses for pediatric and adult patients undergoing CT scans *J. Radiol. Prot.* **35** 891–909
[12] Ding A *et al* 2015 VirtualDose: a software for reporting organ doses from CT for adult and pediatric patients *Phys. Med. Biol.* **60** 5601–25
[13] Tian X, Li X, Segars W P, Paulson E K, Frush D P and Samei E 2014 Pediatric chest and abdominopelvic CT: organ dose estimation based on 42 patient models *Radiology* **270** 535–47
[14] Geyer A M, O'Reilly S, Lee C, Long D J and Bolch W E 2014 The UF/NCI family of hybrid computational phantoms representing the current US population of male and female children, adolescents, and adults—application to CT dosimetry *Phys. Med. Biol.* **59** 5225–42
[15] Lee C, Lodwick D, Hurtado J, Pafundi D, Williams J L and Bolch W E 2010 The uf family of reference hybrid phantoms for computational radiation dosimetry *Phys. Med. Biol.* **55** 339–63
[16] ICRP 2002 Basic anatomical and physiological data for use in radiological protection : reference values *ICRP Publ 89 Ann ICRP.* **32** 1–277
[17] Turner A C *et al* 2010 The feasibility of a scanner-independent technique to estimate organ dose from MDCT scans: using CTDI[sub vol] to account for differences between scanners *Med. Phys.* **37** 1816
[18] Dabin J, Mencarelli A, McMillan D, Romanyukha A, Struelens L and Lee C 2016 Validation of calculation algorithms for organ doses in CT by measurements on a 5 year old paediatric phantom *Phys. Med. Biol.* **61** 4168–82
[19] Giansante L *et al* 2019 Organ doses evaluation for chest computed tomography procedures with TL dosimeters: Comparison with Monte Carlo simulations *J Appl Clin Med Phys.* **20** 308–20
[20] Long D J *et al* 2013 Monte Carlo simulations of adult and pediatric computed tomography exams: validation studies of organ doses with physical phantoms *Med. Phys.* **40** 13901
[21] Lee C, Flynn M J, Judy P F, Cody D D, Bolch W E and Kruger R L 2017 Body size–specific organ and effective doses of chest CT screening examinations of the national lung screening trial *Am. J. Roentgenol.* **208** 1082–8
[22] Johnson P B, Bahadori A A, Eckerman K F, Lee C and Bolch W E 2011 Response functions for computing absorbed dose to skeletal tissues from photon irradiation - an update *Phys. Med. Biol.* **56** 2347
[23] ICRP 2010 Conversion coefficients for radiological protection quantities for external radiation exposures *ICRP Publ 116 Ann ICRP.* **40** 1–258
[24] ICRP 2007 The 2007 Recommendations of the international commission on radiological protection *ICRP Publ 103 Ann ICRP.* **37** 1–332
[25] Narayanan D *et al* 2015 Automated segmentation of the thyroid gland on thoracic CT scans by multiatlas label fusion and random forest classification *J Med Imaging Bellingham Wash.* **2** 044006
[26] Liu J *et al* 2016 Mediastinal lymph node detection and station mapping on chest CT using spatial priors and random forest *Med. Phys.* **43** 4362
[27] Lee C, Liu J, Griffin K, Folio L and Summers R M 2020 Adult patient-specific CT organ dose estimations using automated segmentations and Monte Carlo simulations *Biomed. Phys. Eng. Express* **6** 045016
[28] Li X, Segars W P and Samei E 2014 The impact on CT dose of the variability in tube current modulation technology: a theoretical investigation *Phys. Med. Biol.* **59** 4525–48
[29] Lee E, Lamart S, Little M P and Lee C 2014 Database of normalised computed tomography dose index for retrospective CT dosimetry *J. Radiol. Prot.* **34** 363–88
[30] Nagel H C T 2007 Parameters that influence the radiation dose *Radiation Dose from Adult and Pediatric Multidetector Computed Tomography.* p 51–79
[31] McCollough C *et al* 2014 Use of water equivalent diameter for calculating patient size and size-specific dose estimates (SSDE) in CT: the report of AAPM Task Group 220 *AAPM Rep.* **2014** 6–23 (https://aapm.org/pubs/reports/rpt_220.pdf)
[32] Boone J M, Strauss K J, Cody D D, McCollough C H, McNitt-Gray M F and Toth T L 2011 Size-specific dose estimates (SSDE) in pediatric and adult body CT examinations [Internet] *AAPM* Available from (https://aapm.org/pubs/reports/RPT_204.pdf)
[33] Barreto I, Verma N, Quails N, Olguin C, Correa N and Mohammed T 2020 Patient size matters: Effect of tube current modulation on size-specific dose estimates (SSDE) and image quality in low-dose lung cancer screening CT *J Appl Clin Med Phys.* **21** 87–94
[34] Peng Z *et al* 2020 A method of rapid quantification of patient-specific organ doses for CT using deep-learning-based multi-organ segmentation and GPU-accelerated Monte Carlo dose computing *Med. Phys.* **47** 2526–36